ELSEVIER

Biophysical Chemistry 66 (1997) 57–66

Biophysical Chemistry

Macromolecular crowding: effects on actin polymerisation

Robyn A. Lindner [1], Gregory B. Ralston *

Department of Biochemistry, University of Sydney, Sydney, NSW 2006, Australia

Received 23 September 1996; revised 13 January 1997; accepted 16 January 1997

Abstract

Dextran has been found to enhance the polymerisation of actin. This enhancement increases exponentially with increasing mass concentrations of dextran, in a manner that is consistent with excluded volume theory. Mathematical prediction of experimental results is difficult due to the fact that all participating species, namely F-actin, G-actin and dextran are best represented by differently shaped hard particles. Modelling dextran as a sphere of radius defined by an effective thermodynamic radius (R_{eff}), we have predicted our experimental results to an acceptable degree, given the relative crudity of the model. The results imply that the highly crowded cellular environment may help to stabilise the filamentous actin network in vivo.

Keywords: Actin; Dextran; Macromolecular crowding; Excluded volume

1. Introduction

The red blood cell cytoskeleton is responsible for maintaining the flexibility and durability of the red blood cell. The principal component of the cytoskeleton necessary for maintaining cell integrity is a ternary complex of spectrin, actin and band 4.1 which is linked to other such ternary complexes, forming a two-dimensional network which spans the intracellular side of the lipid bilayer [1]. Haemoglobin occupies around one third of the interior volume of the red blood cell. The result is a highly crowded environment which contrasts with the dilute in vitro conditions under which cellular components are usually studied in the laboratory. Consequently, a study of the interactions between erythroid cytoskeletal elements under crowded conditions is relevant to the conditions under which these proteins associate in vivo. Using dextran to mimic the crowded interior of the red blood cell, it has been shown that dextran enhances erythrocyte spectrin self-association [2]. In an attempt to gain an overall understanding of cytoskeletal interactions in the erythrocyte in vivo, the effects of crowding agents on actin polymerisation have been investigated in this laboratory.

Fluorimetry of *N*-(1-pyrenyl)iodoacetamide labelled-actin [3] has been chosen to study actin polymerisation. This technique is distinguished from other means of measuring actin polymerisation in being highly sensitive to even a small amount of F-actin co-existing with G-actin, thus enabling an accurate

* Corresponding author. Tel.: (61) 2 93513906, fax: (61) 2 93514726, e-mail: g.ralston@biochem.usyd.edu.au

[1] Present address: Department of Chemistry, University of Wollongong, NSW, 2522, Australia.

PII S0301-4622(97)00011-2

and relatively simple determination of the critical concentration of actin compared to other techniques such as viscosity and light scattering [4,5].

The aim of this study is to determine the effects of dextran on actin polymerisation, using fluorimetry, in order to gain a better understanding of actin polymerisation and cytoskeletal interactions under the crowded conditions to be found in vivo.

2. Theory

The equilibrium state of a system is dependent upon the chemical potentials (μ_i) of the products and the reactants present in the system [6]. In an ideal solution (in practice, one in which concentrations are vanishingly dilute) the molar chemical potential μ_i of any species, i, is dependent upon the concentration of the species according to the relationship:

$$\mu_i = \mu_i^\circ + RT \ln c_i \quad (1)$$

where μ_i° is the chemical potential in the standard state, and c_i is the molar concentration of species i. In real solutions, however, the chemical potential differs from the ideal value because of the interactions between molecules of i and other molecules [6]:

$$\mu_i = \mu_i^\circ + RT \ln(\gamma_i c_i) \quad (2)$$

where γ_i is the activity coefficient of i, taking into account all departures from ideal behaviour. The activity coefficient may be expressed as:

$$\gamma_i \equiv \exp(\mu^{NI}/RT) \quad (3)$$

where μ^{NI} may be considered to be the non-ideal component of μ_i [6].

The fact that solute molecules occupy space will result in a decrease in entropy through volume exclusion phenomena, even when direct (such as electrostatic) interactions are absent. As more of the solution volume is occupied by solute molecules, either through increased concentration of the solute of interest, or through addition of otherwise inert 'bystander' molecules, excluded volume effects will increase the activity coefficient of solutes [6]:

$$\ln\gamma_i = \sum_j \alpha_{ij} c_j + \sum_j \sum_k \alpha_{ijk} c_j c_k + \ldots \quad (4)$$

where the α_{ij} are a measure of two-way particle interactions (viz. the volumes of solution excluded to molecule j by molecule i, expressed in l/mol, known as the molar covolume), the α_{ijk} are a measure of three-way interactions, and so on, with the sums extending over all species. The effect of macromolecular crowding on association constants arising from the presence of inert, space-filling molecules has been analysed by Nichol et al. [7]. In the case of a self-association reaction, such as $nA \rightleftharpoons B$, the thermodynamic association constant, K, is given:

$$K = \frac{c_B}{c_A^n} \frac{\gamma_B}{(\gamma_A)^n} = K_{app} \frac{\gamma_B}{(\gamma_A)^n} \quad (5)$$

where K_{app} is the apparent equilibrium constant determined from the equilibrium concentrations. In general, the activity coefficient ratio, $\gamma_B/(\gamma_A)^n$, will not be unity, and the apparent association constant is therefore altered by the existence of nonideality. When the associating molecule is present in low concentrations, and in the presence of relatively high concentrations of inert, space-filling molecules, P, Eq. (4) will be dominated by the contributions of the volume excluded to P by the oligomeric states, and

$$K_{app} = K \exp(-\Delta U c_P) \quad (6)$$

where $\Delta U = (\alpha_{BP} - n\alpha_{AP})$is the change in molar covolume upon association [8], and c_P is the molar concentration of inert bystander molecules or 'crowding agent'.

A determination of the equilibrium constant for actin polymerisation in the presence of dextran will allow a test for the prediction of Eq. (6). Dextran is an uncharged, inert polymer, with excluded volume properties that are independent of pH, salt concentration, absolute protein concentration, and the degree of polymerisation of dextran [9]. The use of dextran in excluded volume studies has been previously reported by a number of researchers [2,10–13].

3. Experimental

3.1. Materials

Fresh rabbits were obtained from butcher shops and were used on the same day as purchased. *N*-(1-

pyrenyl)iodoacetamide was obtained from Molecular Probes (USA). Dextran fractions (weight-average molecular weight 10 000, 40 800, 70 000 and 162 000), polyethylene glycols (weight-average molecular weight 400, 1000 and 3350) and adenosine 5′-triphosphate (disodium salt) (Grade 1, catalog number A-2383) were obtained from Sigma. Dextran (weight-average molecular weight 110 000) was obtained from Pharmacia.

3.2. Preparation of actin

Acetone powder was prepared from rabbit muscle based on the method of Spudich and Watt [14] with the modifications of Eisenberg and Kielley [15]. The dry acetone powder was then stored in an airtight container at −20°C.

Actin was extracted from acetone powder using the method of Pardee and Spudich [16]. Actin was purified further by chromatography at 4°C using a Sephadex G-200 column (2.5 × 48 cm) in order to remove actin-binding proteins which can inhibit formation of actin filament networks [17]. F-actin was stored in F-buffer (2 mM Tris–HCl, pH 7.6, 50 mM KCl, 2 mM $CaCl_2$, 1 mM ATP, 0.5 mM 2-mercaptoethanol, 0.005% NaN_3) for short periods at 4°C. For prolonged periods of storage, F-actin was stored in 50% glycerol at −20°C and subjected to a cycle of depolymerisation and polymerisation prior to use.

3.3. Labelling actin with N-(1-pyrenyl)iodoacetamide

Actin was labelled with *N*-(1-pyrenyl)iodoacetamide using the method of Kouyama and Mihashi [3]. A final ratio of labelled actin : unlabelled actin of 1:6 was used and the labelled sample was diluted with unlabelled F-actin, if necessary, in order to obtain this degree of labelling. The degree of labelling was determined using the following: G-actin has an extinction coefficient of 0.617 $l\,g^{-1}cm^{-1}$ at 290 nm [18] and *N*-(1-pyrenyl)-iodoacetamide-labelled G-actin has an extinction coefficient of 0.512 $l\,g^{-1}cm^{-1}$ at 344 nm [19]. The labelled F-actin pellet was stored at 4°C until required (within days). When required, the pellet was resuspended in F-buffer (2 mM Tris–HCl, pH 7.6, 50 mM KCl, 2 mM $CaCl_2$, 1 mM ATP, 0.5 mM 2-mercaptoethanol, 0.005% NaN_3). The molecular weight for G-actin was taken to be 42 300 [20] for all work presented in this paper.

3.4. Incubation of actin with dextran or polyethylene glycol (PEG)

The concentration of F-actin, labelled with *N*-(1-pyrenyl)iodoacetamide, was determined using an F-actin extinction coefficient of 0.638 $l\,g^{-1}cm^{-1}$ at 290 nm [18]. F-actin was then diluted with F-buffer to a range of actin concentrations from 0.004–0.1 g/l and was incubated in the presence of dextran or PEG over a range of dextran or PEG molecular masses and concentrations. The final volume of samples was 3 ml. Samples were mixed well by inversion and were incubated in the dark for 20 h at 37°C. Time-course studies by Strömqvist et al. [5] indicate that equilibrium is reached in approximately 4 h in the absence of polymers, and that 20 h is sufficient for equilibrium to be reached in the presence of up to 10% (w/v) PEG. The presence of dextran or PEG did not cause any significant change in solution pH.

3.5. Fluorimetry

The fluorescence intensity of the incubated F-actin samples was measured at 37°C using a Perkin Elmer Luminescence Spectrometer LS50. Samples were mixed well by inversion before being placed in the spectrometer cuvette, taking care that any air bubbles were dislodged. An excitation wavelength of 365 nm (slit width 2.5 nm) and an emission wavelength of 386 nm (slit width 4.0 nm) were used [21,22].

3.6. Data analysis: fitting of discontinuous functions to fluorimetry data using non-linear regression

The fitting of two discontinuous functions to fluorescence intensity versus actin concentration data obtained from fluorimetry experiments was necessary in order to determine the critical concentration for actin. Duggleby [23] has developed a model which enables quantitative analysis of two straight lines joined by a transition curve. This formula has been adapted from a general formula by Watts and Bacon [24]. The model consists of a general form of the hyperbola in which two straight lines are connected by a transition curve (see Eq. 1 of ref. [23]).

For the purposes of our studies, the value of the curvature parameter for the transition region is taken as zero, indicating an infinitely sharp transition region which can now be represented by a single point at which the two lines meet. Thus the equation is as follows:

$$y = y_t - \frac{(E_L + E_R)(x - x_t)}{2} + \frac{(E_L - E_R)|x - x_t|}{2} \quad (7)$$

where: y_t = y-intercept value of the point of intersection between the two lines, x_t = x-intercept value of the point of intersection between the two lines, E_L = slope of the line to the left of the point of intersection, E_R = slope of the line to the right of the point of intersection.

This formula was fitted to experimental data by means of non-linear regression (using MacCurveFit 1.0.1; K. Raner, CSIRO) in order to obtain estimates and the approximate standard errors for the 4 parameters. The fitting algorithm used was the Quasi-Newton algorithm and best fits were taken as those which gave a combination of lowest sums of squares of the residuals, and R^2 (coefficient of determination) values closest to 1. The abscissa value of the transition point (x_t) gives the value for the critical concentration for actin.

To ensure that best fits obtained reflected global, rather than local, minima, once a 'best' fit was obtained, estimates for the parameters were inserted that varied considerably from the best fit values and the fitting program was allowed to converge on new minima. This step was performed numerous times; each time different parameter estimates were used lying on either side of the putative best fit values. If parameter values concurred with those of the original fit then we assumed that we had reached a true minimum.

From the critical concentration, the apparent association constant for actin polymerisation was determined using Eq. (8) [25]:

$$K_{ass}^{app} = \frac{1}{C_c} \quad (8)$$

where K_{ass}^{app} is the apparent association constant for actin polymerisation, C_c is the critical concentration for actin polymerisation.

3.7. Atomic absorption spectroscopy

The concentrations of Ca^{2+} and Mg^{2+} in samples of dextran were determined using flame atomic absorption spectroscopy. Dextran samples (30% w/v) were prepared in 0.1% nitric acid in Milli-Q water for dextran MW 10000, 40800, 70000 and 110000. Standard solutions for Mg^{2+} and Ca^{2+} were also prepared in 0.1% nitric acid in Milli-Q water. Standard solutions were prepared in the concentration range of 0–0.5 μg/ml (Mg^{2+}) and 0–5 μg/ml (Ca^{2+}). All sample and standard preparations were performed using glassware that had been washed overnight in 5% nitric acid, followed by 5 washes in reverse osmosis water, and finally in Milli-Q water. Experiments were performed using a Varian SpectrAA-20 plus Atomic Absorption Spectrometer. Dextran samples of MW 70000 and 110000 were diluted to 15% (w/v) for analysis since 30% (w/v) solutions were too viscous to enable easy sampling of the solutions. Ca^{2+} determinations were performed using acetylene and nitrous oxide as the fuel and support respectively. A wavelength of 422.7 nm and a slit width of 0.5 nm were used for data acquisition. For Mg^{2+}, acetylene and air were used as the fuel and support respectively, and data were acquired at 285.2 nm with a slit width of 0.5 nm.

4. Results

4.1. The effect of the mass concentration of dextran on actin polymerisation

The presence of dextran, over a range of concentrations (between 0–15% w/v) and over a range of dextran molecular weights, was found to reduce the critical concentration of actin. Fig. 1 shows results obtained with increasing concentrations of dextran of molecular weight 70000. Similar results were obtained for other sizes of dextran. Comparison of absolute fluorescence intensity data was restricted to experiments performed using actin labelled in the same 'batch' since the degree of labelling varied slightly with each labelling procedure. Direct comparison of absolute fluorescence intensity values was also restricted to experiments performed on the same day to avoid complications from possible breakdown

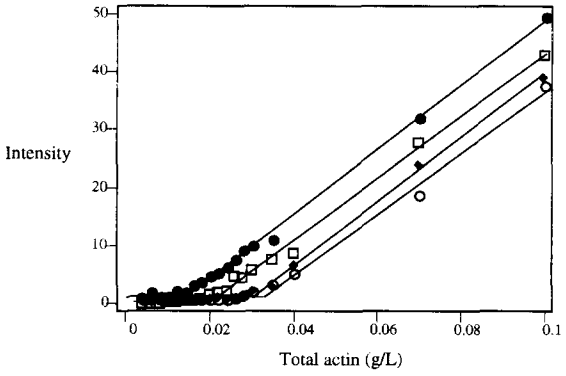

Fig. 1. The effect of dextran on the actin polymerisation. Pyrene-labelled actin, over a range of concentrations, was incubated for 20 h at 37°C in the presence of a range of dextran concentrations (0–15% w/v) and the fluorescence intensity measured as a function of actin concentration. Shown here are the results for dextran of molecular mass 70000. Dextran concentration (%w/v): ○, 0%; ◆, 5%; □, 10%; ●, 15%. The lines represent the fit of Eq. (7) to each set of experimental data values. C_c values (mg/l ± SE) obtained for each dextran concentration are as follows: 0%, 33 ± 1.4; 5%, 31.3 ± 0.8; 10%, 22.8 ± 1.4; 15%, 15.8 ± 1.4.

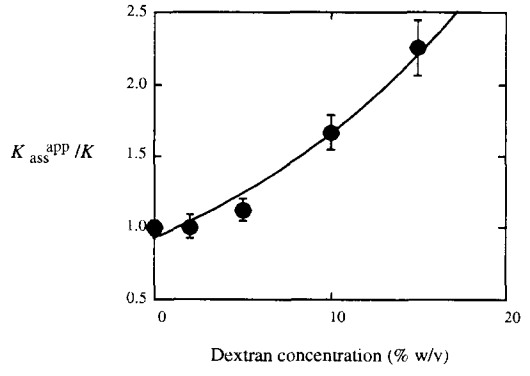

Fig. 2. The effect of mass concentration of dextran on K_{ass}^{app} for a fixed molecular mass of dextran. Data shown here were obtained using dextran MW 110000. The data have been fitted with a single exponential function by means of unweighted linear regression. Approximate standard errors derived from the fitting process are shown.

of the fluorescent label over time. Data were therefore normalised with respect to the control data in order to compare experiments performed on other days and with different batches of actin.

Values for K_{ass}^{app} were determined from the values of C_c (using Eq. (8)) where K_{ass}^{app} is the apparent equilibrium constant for actin polymerisation in the presence of dextran. When K_{ass}^{app}/K is plotted against dextran concentration (where K is equal to K_{ass}^{app} in the absence of dextran) (Fig. 2) we observe that the increase in K_{ass}^{app} appears to be exponential. This is consistent with excluded volume theory (Eq. (6)). Accordingly, the data have been fitted with a simple exponential function. Within the precision of the measurements, the values for K_{ass}^{app}/K appear to be independent of the molecular mass of dextran for a given mass concentration of dextran. This is demonstrated in Fig. 3 which shows that K_{ass}^{app}/K is strongly dependent upon the mass concentration of dextran, yet for a given mass concentration is relatively independent of the molecular mass. K_{ass}^{app}/K data obtained using dextran of MW 162000 was not used for further analysis as the results were poorly reproducible, presumably due to the high viscosities of the higher concentration solutions of this higher molecular weight dextran.

From the graphs of $\ln K_{ass}^{app}/K$ versus dextran concentration, a straight line is obtained, the slope of which is equal to the decrease in molar covolume, ΔU (in units of l/mol) for the association of an actin monomer to an actin filament in the presence of dextran. ΔU increases linearly with increasing dextran molecular weight (shown in Fig. 4), suggesting

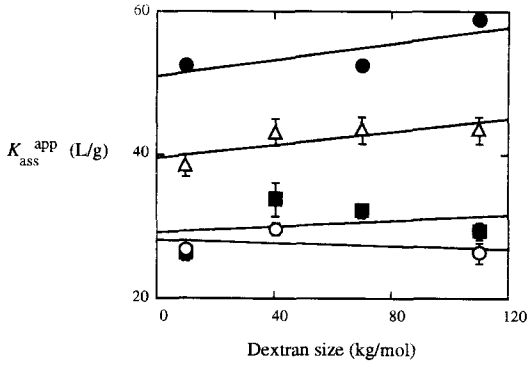

Fig. 3. The effect of dextran MW on K_{ass}^{app} for fixed mass concentrations of dextran. Data were obtained from individual experiments and have been fitted with straight lines by unweighted linear regression. Dextran (% w/v): ○, 2%; ■, 5%; △, 10%; ●, 15%. *t*-tests show that the slopes of these lines are not significantly different from zero ($p > 0.5$). Errors are standard errors derived from the fitting process.

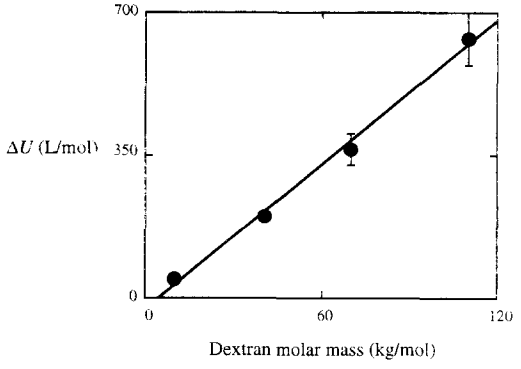

Fig. 4. The dependence of the change in molar excluded volume upon the molar mass of dextran. Values of ΔU (l/mol) were obtained from the slopes of logarithmic plots of K_{ass}^{app}/K versus dextran concentration data. Data have been fitted with a straight line by unweighted linear regression. Error bars represent the standard deviations of the slopes of the logarithmic plots. The slope of the line gives ΔU in units of l/g of dextran. $\Delta U = -5.9 \pm 0.3$ ml/g.

that all the surface of the dextran molecule is accessible to actin, and that dextran behaves as a thread-like molecule to actin. These results are consistent with those obtained for the self-association of spectrin in the presence of dextran [2].

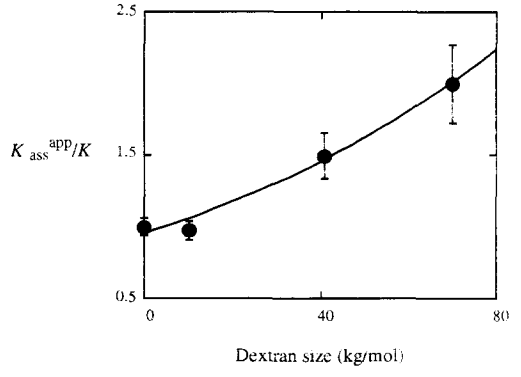

Fig. 5. The effect of the molar mass of dextran on K_{ass}^{app} for a fixed molar concentration of dextran. The value of K_{ass}^{app} was estimated for pyrene-labelled F-actin in the presence of a range of dextran sizes, all at a fixed molar concentration of 2 mM. Data have been fitted with a single exponential function by means of unweighted linear regression. Error bars represent standard errors derived from the fitting process. No dextran greater than MW 70000 was used as 2 mM solutions of higher molecular weight dextrans were too viscous to produce reproducible results.

4.2. Effect of dextran molecular weight on K_{ass}^{app} for a fixed molar concentration of dextran

In order to confirm our finding that ΔU (in units of l/mol) increases linearly with increasing dextran size, we set out to measure the effect of dextran size on K_{ass}^{app} for a *fixed molar* concentration of dextran. Actin was incubated at 37°C with a range of different dextran molecular weights, all at a fixed concentration of 2 mM (based on the weight-average molecular weight of dextran). At a fixed molar concentration of dextran, K_{ass}^{app}/K increases exponentially with increasing dextran molecular weight (Fig. 5). This confirms that the change in molar covolume upon association of actin monomer to an actin filament is linearly dependent upon dextran size. As a consequence, the change in covolume in units of l/g will be independent of the molar mass of dextran.

4.3. The effect of polyethylene glycol on actin polymerisation

F-actin was incubated in the presence of a range of concentrations and molecular weights of polyethylene glycol (PEG). PEG (MW 3350) (over a range of mass concentrations) was found to reduce the critical concentration of actin. The subsequent enhancement of K_{ass}^{app} was found to be exponential with increasing PEG concentration (Fig. 6).

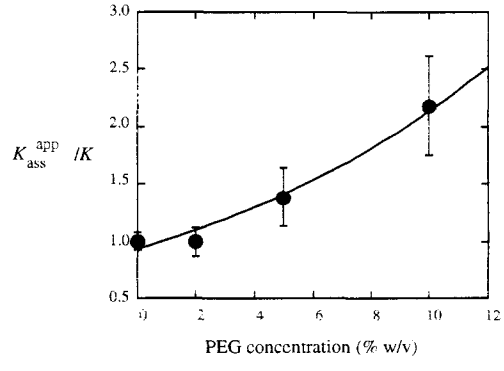

Fig. 6. The effect of increasing mass concentrations of polyethylene glycol (PEG) 3350 on K_{ass}^{app}/K for actin polymerisation. F-actin (0.004–0.1 g/l) was incubated for 20 h at 37°C in the presence of 0, 2, 5 and 10% PEG. Data have been fitted with a single exponential function by means of a linear regression. Standard errors shown are derived from the fitting process.

The effect of the molecular weight of PEG on actin polymerisation was studied for a fixed mass concentration of PEG (10% w/v) for two fractions of PEG: PEG MW 400 and 3350. Both PEG 400 and 3350 were observed to reduce the C_c of actin.

4.4. Determination of Ca^{2+} and Mg^{2+} concentrations in dextran

Atomic absorption spectroscopy failed to detect any Ca^{2+} or Mg^{2+} in dextran solutions over the cation concentration ranges of 0–0.125 mM and 0–0.02 mM, respectively. These results were obtained at concentrations of dextran equal to, or greater than, the maximum concentration used for experiments in this work. The lowest concentration standards used were 0.025 mM and 0.004 mM for Ca^{2+} and Mg^{2+}, respectively. These concentrations correspond to the highest cation concentrations that may be present in the dextran solutions analysed. Actin polymerisation studies were performed in the presence of 2 mM added Ca^{2+}. Therefore, at the low levels that these cations could be present in dextran, any Ca^{2+} or Mg^{2+} present in the dextran samples will not have contributed significantly to the divalent cation concentration of the actin buffer solution. Consequently, increased levels of Ca^{2+} or Mg^{2+} arising from dextran samples can be eliminated as a reason for enhanced actin polymerisation in the presence of increasing concentrations of dextran.

5. Discussion

5.1. The effect of dextran on actin polymerisation

Dextran was found to enhance the polymerisation of actin in a manner consistent with excluded volume theory. The decrease in C_c for actin polymerisation in the presence of increasing concentrations of dextran is consistent with results obtained by others in the presence of PEG [5,26]. Both groups [5,26] found that PEG accelerates the rate, and increases the extent of actin polymerisation but, in contrast to our work, these studies were restricted to only one size fraction of polymer. These effects of PEG were attributed to excluded volume phenomena [5,26]. Tellam et al. [26] have presented a simplified mathematical model (based on excluded volume theory) which predicts their experimental results. Numerous other studies have been performed on the effects of macromolecules on actin polymerisation behaviour [27–29]. In all the above-mentioned cases, researchers have noted that the observed effects may more realistically represent what is happening in vivo than more typical 'dilute' in vitro experiments.

The exponential enhancement of K_{ass}^{app}/K for actin polymerisation (Fig. 2) with increasing mass concentrations of dextran is consistent with excluded volume theory, indicating that a loss of excluded volume occurs when an actin monomer associates with an actin filament in the presence of dextran. As a result, in a crowded environment as occurs in vivo, the degree of association of actin may be higher than predicted from dilute solutions. The implication from this is that the highly crowded cellular environment may serve to stabilise the F-actin filament in vivo and may, in turn, help to stabilise the cytoskeletal network.

The decrease in molar covolume for actin polymerisation in the presence of a given mass concentration of dextran, ΔU (in units of l/mol), is approximately linearly dependent upon dextran molecular weight. This result is similar to that obtained for the effect of dextran on the self-association of spectrin dimers [2]. This linear dependence implies that to actin, dextran appears as a thread-like molecule which has most of its surface area available to the actin molecule. Dextran is perhaps best modelled as a branched random coil but may be sufficiently extended such that most of its surface is penetrable to the actin monomer and filament [30].

5.2. Prediction of the effects of dextran on actin polymerisation using mathematical models

Prediction of our experimental results is complicated by the fact that all of the participating species are best represented by differently shaped hard particles: F-actin is rod-like, G-actin is globular, and dextran is randomly coiled. The problem of modelling this interaction is intractable without some degree of simplification or compromise.

Tellam et al. [26] modelled F-actin as an end-to-end, linearly associating chain of spherical monomers, and estimated the change in molar covol-

ume for the polymerisation of actin in the presence of PEG (modelled as a rigid sphere). This change in covolume is defined as:

$$\Delta U = -2N\pi r^2(3a + 2r)/3 \quad (9)$$

where: N = Avogadro's number, a = radius of the actin monomer, r = radius of the equivalent sphere model for the inert polymer.

To apply this model to our data requires an approximation of dextran as a hard sphere, which contradicts experimental findings. However, absence of a more realistic model has led us to adapt the model of Tellam et al. [26] to predict our experimental results.

Tellam et al. [26] modelled PEG as a hard sphere of radius equal to the Stokes radius. Rather than use a hydrodynamic dimension for the representation of dextran as a hard sphere, it was preferable for us to represent dextran as an effective hard sphere, for which the thermodynamic radius would be specific for the relationship between dextran and actin, and would take into account all possible orientations of the dextran molecule with respect to actin. In order to determine the effective radius of an equivalent hard sphere of dextran with respect to actin, we used the model of Jansons and Phillips [31].

$$U = \frac{2}{3}\pi RL^2 + 4\sqrt{\frac{2\pi}{3}}R^2L + \frac{4}{3}\pi R^3 \quad (10)$$

where: U = the volume excluded to a spherical molecule by a Gaussian chain, R = radius of the sphere, L = root mean square end-to-end distance of the Gaussian chain.

This model enables the estimation of the volume excluded to a quasi-spherical protein, such as G-actin, by a randomly coiled polymer, such as dextran and polyethylene glycol. Wills et al. [32] have found that this relationship gives a good fit to experimental data when the globular protein is modelled as an effective sphere (using R = Stokes radius) and the polymer as an effective Gaussian chain (L = root mean square end-to-end distance). Using a Stokes radius for actin of 2.15 nm [26], and the root mean square end-to-end distance for dextran (L) ($L = \sqrt{6}\ R_g$ where $R_g = 0.66M^{0.43}$, [33]), the volume excluded by dextran to actin was determined using Eq. (10). This excluded volume takes into account all possible orientations that the dextran molecule may have with respect to the actin molecule. The effective radius (R_{eff}) of an equivalent hard sphere model for dextran that gives an excluded volume estimation equivalent to that obtained from Jansons and Phillips model was then determined using the following:

$$R_{eff} = \sqrt[3]{\frac{3U}{4\pi}} - a \quad (11)$$

where: U = the volume excluded by dextran to actin determined using Eq. (10), a = radius of an actin monomer (21.5 Å [26]).

The change in excluded volume for actin polymerisation in the presence of dextran (ΔU) was then estimated using Tellam's [26] model (Eq. (9)) with the radius of dextran defined by R_{eff}. The values for ΔU determined for a range of dextran molecular weights are shown in Table 1.

Table 1 shows a relative independence of the predicted ΔU (in units of ml/g) upon dextran molecular weight, in agreement with our experimental findings. It appears from Table 1 that the model used here results in an overestimate of the experimentally determined value for ΔU. This is most probably due to the fact that the spherical model used for dextran is inappropriate. Mathematical simulations using the Janson and Phillips model show an almost linear relationship between dextran size and U (Fig. 7) indicating an extended structure for dextran as opposed to a compact, spherical one. Only at low dextran molecular weights does this relationship between U and molecular weight deviate markedly from linearity as the dextran becomes small in com-

Table 1
The change in covolume (ΔU) for the polymerisation of actin in the presence of dextran

Dextran MW	ΔU (theoretical)		ΔU (experimental)	
	(l/mole)	(ml/g)	(l/mole)	(ml/g)
10000	−148	−14.8	−46.4±8.7	−4.6±0.8
40000	−439	−11.0	−201±7.0	−4.9±0.2
70000	−849	−12.1	−365±39	−5.2±0.6
110000	−1270	−11.5	−636±66	−5.8±0.6

Values were determined both experimentally by fluorimetry, and theoretically using a combination of the models of Jansons and Phillips [31] and Tellam et al. [26]. Errors represent the standard deviations as shown in Fig. 4.

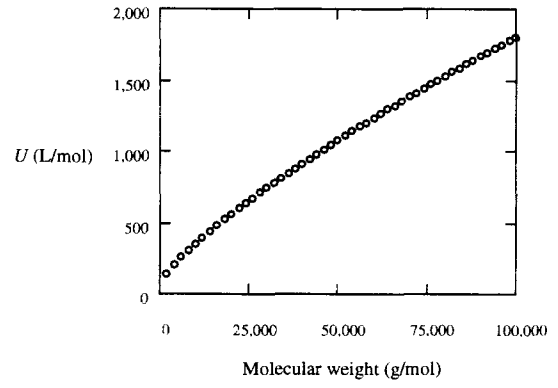

Fig. 7. Simulation showing the dependence of excluded volume (U) on dextran molecular weight for a spherical protein of radius equal to 21.5 Å (equivalent to monomeric actin) using the model of Jansons and Phillips [31] (Eq. (10)). The relationship is approximately linear for larger dextrans. Simulations were performed with the aid of Mathematica.

parison to the size of the protein and thus approaches a spherical conformation relative to the protein. Dextran, modelled as a sphere, will be less able to penetrate the interstices between actin molecules within the filament; consequently, upon association, the predicted loss in the volume excluded to a spherically modelled dextran molecule will be greater than that excluded to a randomly coiled model. Another factor which should be noted is that a single R_{eff} value for dextran used in these calculations may not be appropriate. The effective radius of dextran towards globular G-actin may be quite different to that towards rod-like F-actin.

The predicted values for ΔU are acceptable given the compromises made in modelling dextran as an effective sphere, and the relative crudeness of the model. The model of Tellam et al. [26] assumes an end-to-end linearly associating chain of actin monomers, with each monomer coming into contact with only one monomer within the chain upon association. F-actin is a helical polymer [34]. Each actin monomer added to the helical filament comes into contact with at least two other monomers within the chain. An assumption is also made in Tellam's model that monomeric actin, and those monomers existing at the ends of the filament are equally capable of penetrating the dextran molecule. In reality, this is highly unlikely given that while the actin monomer may be approximated by a sphere of radius 2.15 nm, the average actin filament is a rod-like structure of 36 nm/turn long and 9–9.5 nm diameter [35], i.e., it is considerably 'thicker' than the globular monomer. The problem is, however, unresolvable without these simplifications.

Dextrans are not monodisperse, and the quoted molecular weights represent the weight-average molecular weights of dextran fractions. Nevertheless, the present study has shown that, over a more than ten-fold range of weight average molecular weights, for a given mass concentration, the effectiveness of dextran as a space-filling agent is relatively insensitive to molecular weight.

5.3. Estimations of crowding effects in vivo

The enhancement of actin polymerisation and spectrin self-association [2] by dextran suggests a possible stabilising role for crowding agents in stabilising the junctional network within the red cell cytoskeleton. Estimations of the effects of haemoglobin, at physiological concentrations, upon actin polymerisation (using Eq. (9) and a radius for haemoglobin of 31 Å) predict that haemoglobin will have at least a 2-fold enhancement effect upon the association constant for actin polymerisation in vivo. This estimate of the degree of enhancement will underestimate the effect of haemoglobin, since it ignores interaction coefficients beyond the second order. At the high concentrations of haemoglobin present in vivo, higher order interaction coefficients are necessary to adequately predict excluded volume effects.

Acknowledgements

This work was supported by a grant from the Australian Research Council, and from the University of Sydney. The award of an Australian Postgraduate Research Award to RAL is gratefully acknowledged. We thank Dr. Peter Wills for some helpful discussions.

References

[1] T.J. Byers, D. Branton, Proc. Natl. Acad. Sci. USA 82 (1985) 6153.

[2] R. Lindner, G.B. Ralston, Biophys. Chem. 57 (1995) 15.
[3] T. Kouyama, K. Mihashi, Eur. J. Biochem. 114 (1981) 33.
[4] L.S. Tobacman, E.D. Korn, J. Biol. Chem. 258 (1983) 3207.
[5] M. Strömqvist, L. Backman, V.P. Shanbhag, J. Mus. Res. Cell Motil. 5 (1984) 443.
[6] A.P. Minton, Mol. Cell. Biochem. 55 (1983) 119.
[7] L.W. Nichol, A.G. Ogston, P.R. Wills, FEBS Lett. 126 (1981) 18.
[8] P.R. Wills, W.D. Comper, D.J. Winzor, Arch. Biochem. Biophys. 300 (1993) 206.
[9] T.C. Laurent, Biochem. J. 89 (1963) 253.
[10] T.C. Jarvis, D.M. Ring, S.S. Daube, P.H. von Hippel, J. Biol. Chem. 265 (1990) 15160.
[11] S.B. Zimmermann, S.O. Trach, Nucleic Acids Res. 16 (1988) 6309.
[12] S.B. Zimmermann, S.O. Trach, Biochim. Biophys. Acta 949 (1988) 297.
[13] L.W. Nichol, M.J. Sculley, L.D. Ward, D.J. Winzor, Arch. Biochem. Biophys. 222 (1983) 574.
[14] J.A. Spudich, S. Watt, J. Biol. Chem. 246 (1971) 4866.
[15] E. Eisenberg, W.W. Kielley, J. Biol. Chem. 249 (1974) 4742.
[16] J.D. Pardee, J.A. Spudich, Meth. Enzymol. 85 (1982) 164.
[17] S. MacLean-Fletcher, T.D. Pollard, Biochem. Biophys. Res. Comm. 96 (1980) 18.
[18] S.L. Brenner, E.D. Korn, J. Biol. Chem. 255 (1980) 1670.
[19] J.A. Cooper, T.D. Pollard, Meth. Enzymol. 85 (1982) 182.
[20] M. Elzinga, J.H. Collins, W.M. Kuehl, R.S. Adelstein, Proc. Natl. Acad. Sci. USA 70 (1973) 2687.
[21] R. Tellam, C. Frieden, Biochemistry 21 (1982) 3207.
[22] L. Tilley, G. Ralston, Biochim. Biophys. Acta 790 (1984) 46.
[23] R.G. Duggleby, Comput. Biol. Med. 14 (1984) 447.
[24] D.G. Watts, D.W. Bacon, Technometrics 16 (1974) 369.
[25] F. Oosawa, S. Asakura, (Eds.). In: Thermodynamics of the Polymerization of Protein, Academic Press, London, 1975, p. 25.
[26] R.L. Tellam, M.J. Sculley, L.W. Nichol, P.R. Wills, Biochem. J. 213 (1983) 651.
[27] J.L. Walsh, H.R. Knull, Biochim. Biophys. Acta 952 (1987) 83.
[28] A. Suzuki, M. Yamazaki, T. Ito, Biochemistry 28 (1989) 6513.
[29] D. Drenckhahn, T.D. Pollard, J. Biol. Chem. 261 (1986) 12754.
[30] J. Hermans, J. Chem. Phys. 77 (1982) 2193.
[31] K.M. Jansons, C.G. Phillips, J. Coll. Interface Sci. 137 (1990) 75.
[32] P.R. Wills, Y. Georgalis, J. Dijk, D.J. Winzor, Biophys. Chem. 57 (1995) 37.
[33] F.R. Senti, N.N. Hellman, N.H. Ludwig, G.E. Babcock, R. Tobin, C.A. Glass, B.L. Lamberts, J. Polym. Sci. 17 (1955) 52.
[34] E.H. Egelman, N. Francis, D.J. DeRosier, Nature 298 (1982) 131.
[35] K.C. Holmes, D. Popp, W. Gebhard, W. Kabsch, Nature 347 (1990) 44.